4 SURFACE CRACK CHARACTERIZATION

The surface of the grout monolith is extensively cracked (Figure 3-1), ranging from large-aperture, curvilinear, radially oriented cracks to small-aperture linear cracks. Most of the cracks had developed by 5 April 2010, when the grout monolith was first uncovered after a month of cure time (Walter et al., 2010, Figure 3-23). A few cracks developed in response to coring that took place later in 2010 and 2011. The initial cracks had apertures up to 5 mm [0.2 in].

Probing large-aperture, curvilinear, radially oriented cracks (sometimes oriented subparallel to the direction of grout flow) indicated this type terminates at the bottom of the third pour of the final lift (Walter, et al., 2010). The pour layer in which these cracks occur was from a batch to which extra water was added onsite to increase grout flowability, but even then the grout was not self-leveling. Because the grout was commonly not self-leveling, it did not always spread uniformly throughout the tank, even though the various batches met slump flow specifications (Walter et al., 2010, Section 3.3). Thus, individual pours varied in volume, thickness, and topography.

Walter, et al., (2010, Figure 3-10) first measured the topography of the grout surface with a laser scanner mounted on a ground-based tripod, such that it scanned the grout surface at a shallow angle and from a single position. The center of the grout monolith was approximated to be 20 cm [8 in] higher than the lowest point in the northeast quadrant of the tank. The initial laser scanner topographic dataset was improved upon by installing a temporary scaffold (Figure 4-1) on both the east and west ends of the tank, in line with the angle-iron crossbeam that joins the tank halves together (cf. Walter, et al., 2010), such that topographic laser scanner data could be collected from two high-angle perspectives in 180° opposition to minimize blind spots caused by the tank wall. These topographic data were brought into an ArcGIS® database for analysis along with carefully mapped crack aperture distributions for all visible surface cracks.

SwRI staff further characterized the 218 surface cracks on the monolith by mapping their locations (Figure 4-2) and apertures (Figure 4-3). Cracks are distributed in fairly distinct sets, including (i) radial to the monolith, (ii) roughly perpendicular to lobe flow fronts, (iii) two *en echelon* bisecting cracks, and (iv) a few cracks/crack families concentric to the monolith edge (Figure 4-2). Cracks that are roughly perpendicular to lobe flow fronts (and thus are roughly orthogonal to surface ripples within the grout flow lobe) commonly terminate between 0 and 10 cm [0 and 25 in] behind the front of the lobe, but occasionally penetrate though the front of a lobe into the underlying grout layer. As such cracks approach the tank liner wall, they are observed to be oriented roughly perpendicular to the wall, similar to the set of radial cracks (Figure 4-2). Aperture varied from <0.5 to 8 mm [<0.02 to 0.31 in], with variation in aperture along crack length (Figure 4-3). Aperture values of at least 4 mm [0.16 in] were found in each quadrant of the monolith.

Crack frequency varies, ranging from 1 to 26 cracks per square meter [9.3×10^{-2} to 2.4 cracks per square foot] (Figure 4-4). Crack frequency is highest along the crossbeam and within the mounded grout flow lobes.

Using the improved topographic dataset, the center of the grout monolith is found to be 21.9 cm [8.6 in] higher than the lowest point in the northeast quadrant of the tank (Figure 4-5). The angle-iron crossbeam may have influenced the degree to which the grout was able to self-level within the final pour of Lift 3. Topography shows some correlation to crack distribution, where cracks are more frequent in areas of higher topography (Figure 4-5). Slope values derived from

Figure 4-1. A Scaffold-Mounted Laser Scanner at the East End of the Intermediate-Scale Grout Monolith Was Used To Measure Surface Topography

the topography data show less correlation to crack distribution (Figure 4-6). Many cracks terminate at or near the edge of a mounded grout flow lobe.

Overcore 9 (Figures 3-1 and 3 -7) sampled the intersection of the two narrow, linear, *en echelon* cracks that vertically dissect the specimen into nearly two equal halves (Figure 4-2). These two *en echelon* cracks are different from the crack sets that are radial to the monolith and roughly perpendicular to lobe flow fronts in their (i) narrower aperture (Figure 4-3), (ii) linearity (Figure 4-2), (iii) vertical orientation (Figure 3-7), (iv) tracelength (Figure 3-7), and (v) development time (Figure 3-7). Inspection of Core 2 during fiscal year 2010 showed that the northeastern *en echelon* crack (Figure 4-2) extended to a depth of at least 61 cm [24 in] below the grout surface. Inspection of Core 9 showed that the longer of the two *en echelon* cracks at this position extended the full length of the core {77 cm [30.3 in]}. Cross-cutting relationships observed in Overcore 9 illustrate that the *en echelon* cracks at this position developed after the shallower subvertical cracks.

Figure 4-2. Photomosaic of the 6.1-m [20-ft]-Diameter Intermediate-Scale Grout Monolith With Crack Distribution Patterns Traced and Coreholes 1–6 Shown. Yellow Cracks Belong to the Set That I Radial to the Monolith, Orange Cracks Belong to the Set That Is Perpendicular to Lobe Flow, Red Cracks Are Two Major *En Echelon* and Several Related Minor Cracks, and Purple Cracks/Crack Families Developed Late Through Coreholes 3 and 5 Concentric to the Monolith Edge.

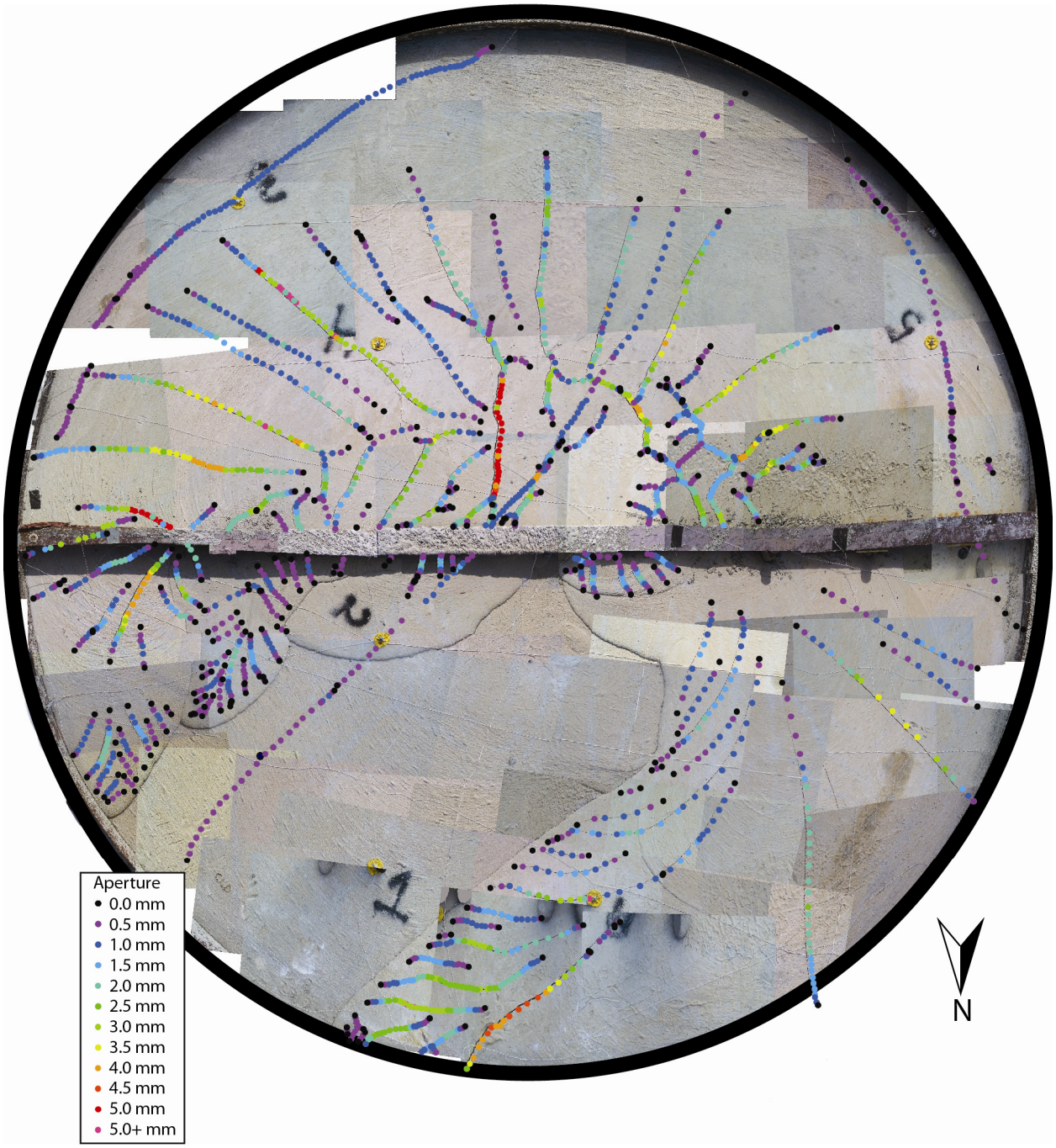

Figure 4-3. Photomosaic of the 6.1-m [20-ft]-Diameter Intermediate-Scale Grout Monolith Draped With Aperture Values Measured Along Its Surface Cracks

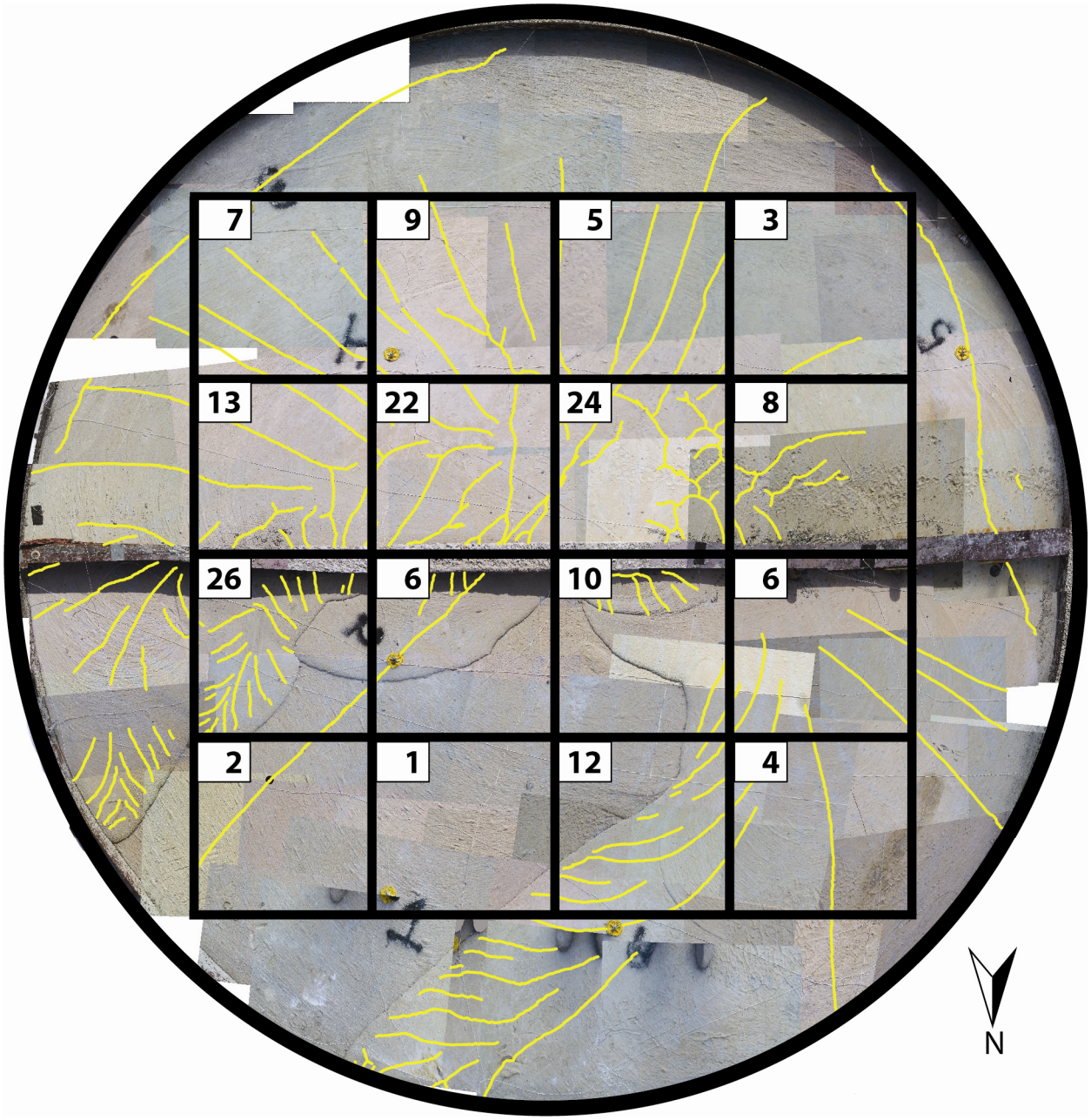

Figure 4-4. Photomosaic of the 6.1-m [20-ft]-Diameter Intermediate-Scale Grout Monolith With Measurement Grid Used To Determine the Surface Crack Frequency Distribution. Number Inside Boxes Represents the Number of Cracks per Square Meter.

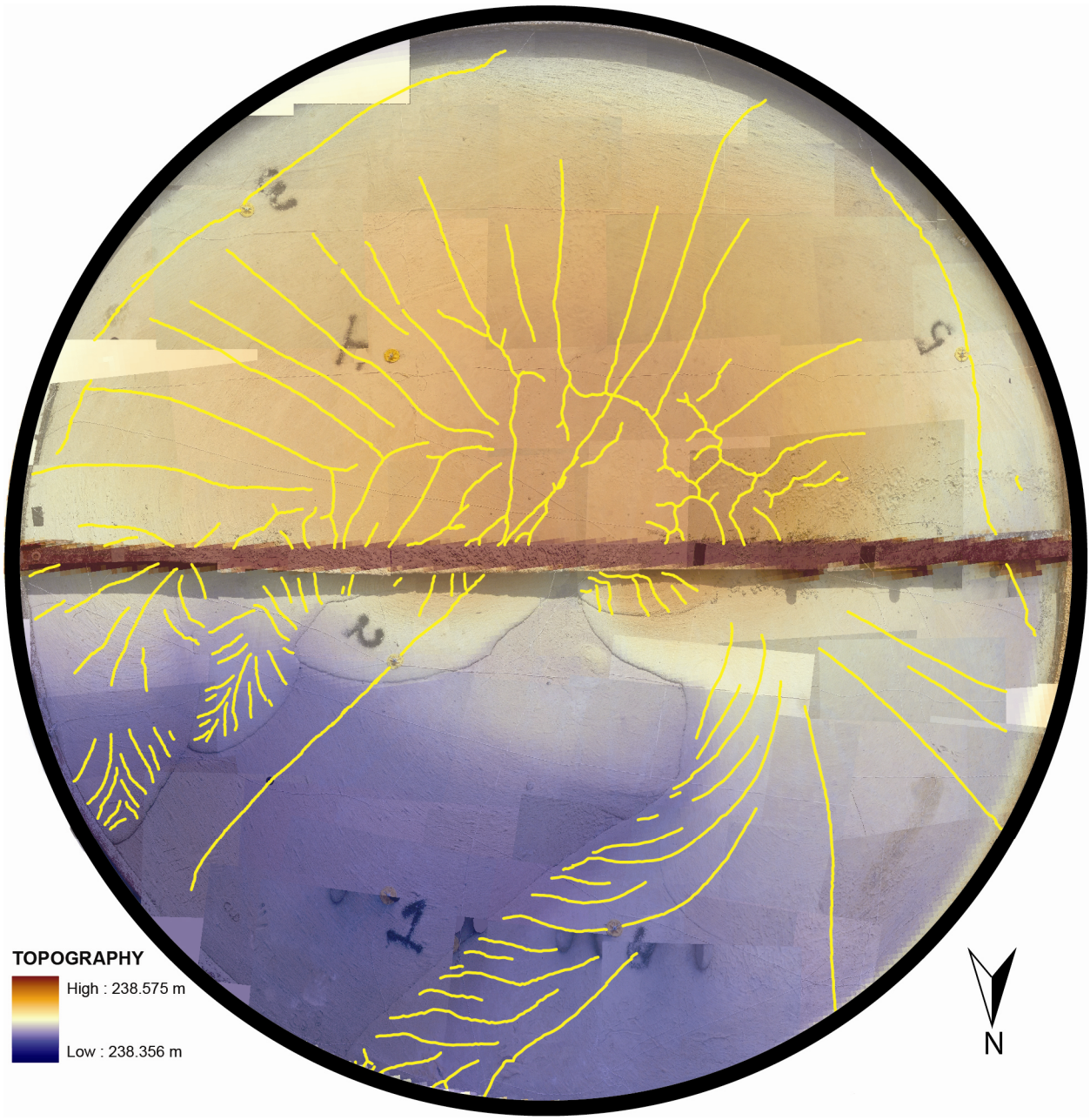

Figure 4-5. Photomosaic of the 6.1-m [20-ft]-Diameter Intermediate-Scale Grout Monolith Draped With a Topographic Map. High to Intermediate Topography Is Represented by Reds to Yellows; Low Topography Is Represented by Shades of Blue.

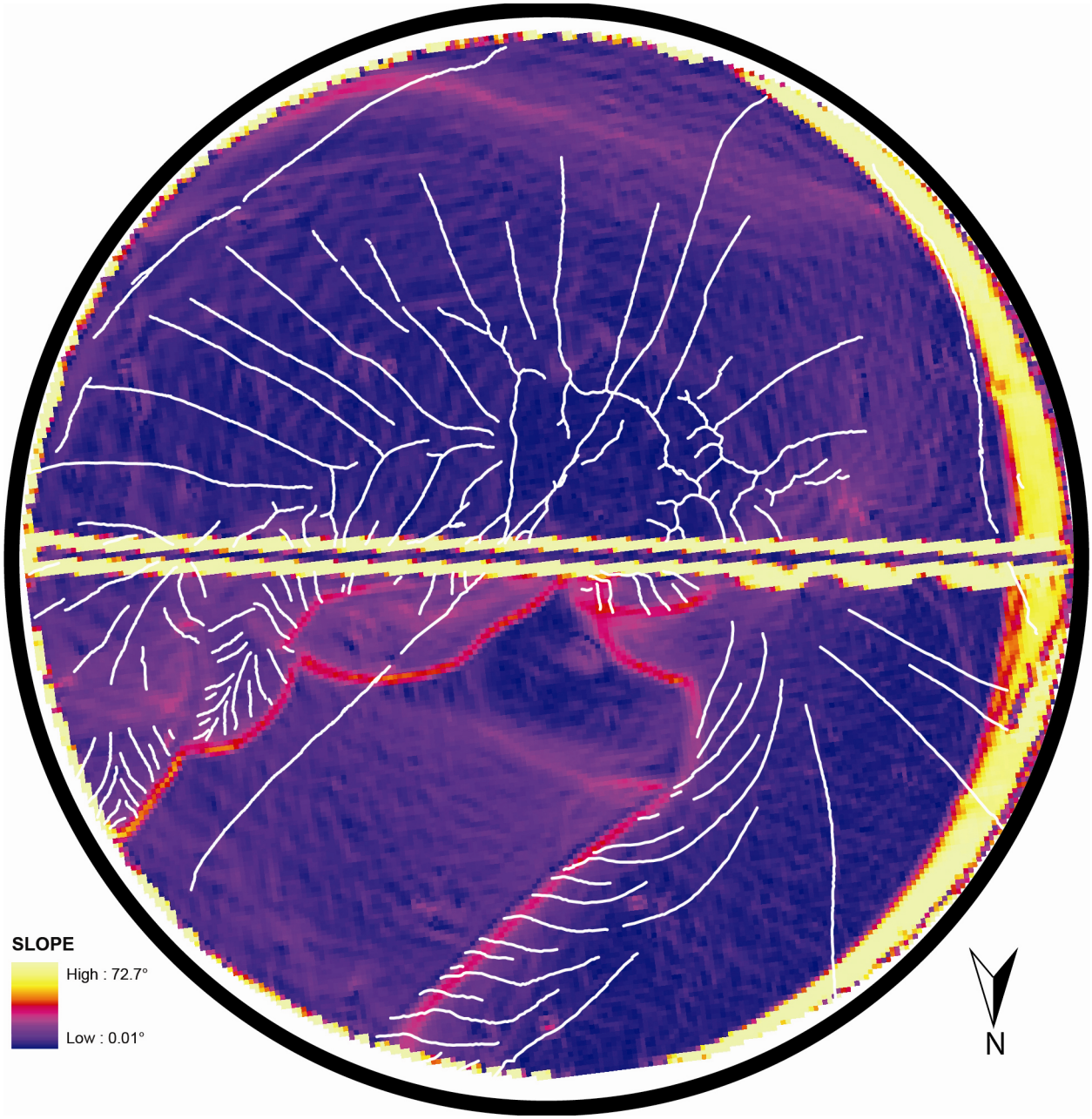

Figure 4-6. A Slope Map of the 6.1-m [20-ft]-Diameter Intermediate-Scale Grout Monolith With Crack Distribution Patterns in White. Steep Slopes Are Represented by Reds to Yellows; Shallow Slopes Are Represented by Blues to Purples. Bright White and Yellow Values Are Artifacts Caused by the Vertical Tank Liner Walls and the Crossbeam.

5 REVIEW OF CRACKING MECHANISMS IN GROUT MONOLITHS AND INTERPRETATION OF CRACKS OBSERVED IN GROUT SPECIMENS

This chapter describes the mechanisms that may lead to cracks in cementitious grout (Table 5-1) used to fill tanks and vaults at NDAA sites. Macroscopic cracks or lack thereof observed in grout monoliths of various sizes and shapes prepared during earlier CNWRA experiments (Walter, et al., 2009, 2010) are then interpreted in terms of these cracking mechanisms.

Concrete literature is vague regarding measureable crack characteristics that would allow definitive determination of cracking mechanisms, and some cracks may reflect a combined response to more than one cracking mechanism.

5.1 Plastic Shrinkage, Plastic Settlement, and Presetting Cracking

Plastic shrinkage, plastic settlement, and presetting (Table 5-1) are terms used by Neville (1996) that are related to contraction due to early water loss (i.e., evaporation from a free surface).

5.2 Hydration and Drying Shrinkage Cracking

Hygral shrinkage (Table 5-1) during curing and drying of a cementitious mass leads to internal stresses that can result in crack formation. Hydration and drying shrinkage occurs during the curing process by incorporation of water molecules into the mineral structure of the cement paste and by loss of water to evaporation at the concrete surface. Such shrinkage decreases with aggregate content and increases with initial water content of the cementitious material.

Table 5-1. Cracking Mechanism Types, Causes, Morphology, and Timing

Mechanism	Cause	Morphologic Characteristics	Timing of Formation
Plastic shrinkage	Contraction due to water loss from surface	Large aperture, long or short	Early
Plastic settlement	Contraction due to non-uniform settlement over obstructions	Undefined	Early
Presetting cracks	A large horizontal area of concrete makes contraction in the horizontal direction more difficult than in the vertical direction	Deep? irregular pattern	Early
Hydration shrinkage (also referred to as hygral or drying shrinkage)	Contraction due to water loss by hydration of cement	Undefined	Middle to late
Thermal stress (also referred to as thermomechanical)	Restrained expansion with heating, followed by contraction with cooling	Small aperture? long length	Middle to late
Other mechanical stress cracks	Extensional strain not related to water loss or temperature	Undefined	Middle to late

The shrinkage factor based on a linear change per unit length basis is typically much larger than the coefficient of thermal expansion for cementitious materials. Shrinkage factors as large as 4,000 x 10-6 have been reported for cement paste (Neville, 1996). Neville (1996) also reports data showing an approximately linear reduction in the shrinkage factors with increasing aggregate content down to approximately 800×10^{-6} at 60 percent aggregate. As Neville (1996) summarized, the amount and effect of shrinkage is not solely a property of the material, but is strongly influenced by the size and shape of the cementitious structure. Drying shrinkage is commonly of minor importance to formation of cracks in massive concrete infrastructure (Springenschmid, 1994), but this may be due to common use of vibrating or other leveling and compaction mechanisms that have no bearing on the NDAA tank closure case.

5.3 Thermomechanical Cracking

Heat of hydration and resultant large temperature gradients within massive concrete infrastructure (both reinforced and unreinforced) are of primary importance to restraint stresses and the formation of cracks (Springenschmid, 1994). Neville (1996) reports a general observation that a temperature difference between the interior and surface of a concrete structure greater than 20 °C [36 °F] can lead to cracking. This observation is based on the coefficient of thermal expansion and tensile strength of concrete, but it may not directly apply to the grout formulations being considered for NDAA tank closures due to the difference in material properties of construction concrete and grout.

Low-heat Portland cement (Type IV) is commonly used in the design of massive structures (Yamazaki, et al., 1995; Ojovan and Lee, 2005) to minimize temperature gradients and cracking potential at early ages, but is not normally used in the immobilization of low- and intermediate-level radioactive waste (Ojovan and Lee, 2005), probably due to the relatively small sizes of these cementitious waste forms. NDAA tank-waste-stabilizing grout monoliths, on the other hand, are of sufficient size that use of Type IV Portland cement might be considered along with any other required special properties to arrive at final recipes for stabilizing grout mixtures. Among its advantages, low-heat Portland cement also slowly develops a higher ultimate compressive strength with increasing age (Yamazaki, et al., 1995).

Little information was found on the thermal properties of grout-type materials. Most of the literature surveyed was related to the thermal conductivity of superplasticized grout used to seal boreholes and pipes for geothermal heat pump systems. Allan (2000) reported the coefficient of thermal expansion of superplasticized cement-sand grout formulation designed for sealing such pipes was 1.65×10^{-5}/°C [0.92×10^{-5}/°F], approximately 60 percent greater than that of typical construction concrete and similar to neat cement (Neville, 1996). Thus, grout may be more susceptible to thermomechanical cracking (Table 5-1) than construction concrete.

5.4 Other Mechanical Stress-Induced Cracking

Bernander and Emborg (1994) pointed out that while thermally induced stresses may contribute to cracking in massive concrete structures, cracking is also influenced by the internal and external constraints on the structure; that is, the boundary conditions that restrain the structure during the thermal expansion stage. They contend that in well-constrained structures, expansion cracks that form during the heating phase tend to close as the structure cools and to not be throughgoing. Cracks that form during the cooling phases, however, tend to remain open and be throughgoing.

Cracks can also be created by external stresses after the structure has cooled, such as ground settling, deformation of bounding constrains, and seismically induced stresses. Whether or not such external factors would be important at the NDAA tank sites is uncertain.

5.5 Interpretation of Cracks Observed in Grout Specimens

5.5.1 Horizontal Cracks

A horizontal parting may demarcate the location of a lift interface or a hiatus between pours of a single lift, especially if relatively planar and all other available evidence suggests the parting formed early. Horizontal partings that consist of two cracks (e.g., Figure 3-7c) that formed subsequent to other cracks, suggest they are not necessarily a lift interface. Horizontal partings tended not to fill with epoxy, perhaps due to very small apertures kept nearly closed by the force of gravity acting on overburden. Water breakthrough patterns on the exposed grout sidewalls during coring operations (Figures 3-2, 3-3a,b) suggest, however, that lift interfaces strongly conduct water through the intermediate-scale grout monolith. There is evidence of a temporal hiatus between the first and second pours within Lift 3 (Figure 3-8) in the Section Three wall exposure. This temporal hiatus is not observed in Lift 3 of Section One (Figure 3-8), which is interpreted as evidence that Pour 1 of Lift 3 did not spread evenly on the surface of Lift 2, but rather piled up in the Section Three wall vicinity locally and is not present in Section One. This interpretation is supported by the distribution of grout shown in Walter, et al., [2010, Figure 3-8(a)].

5.5.2 Shallow, Relatively Large-Aperture, Subvertical Cracks, and Matrix Color

Hydration and drying shrinkage cracking increases with initial water content of cementitious material. The nominal water-to-cement ratio for Local Reducing Grout is ≤0.38, and the intermediate-scale grout monolith batches of Local Reducing Grout ranged from 0.29 to 0.33 (Walter, et al., 2010)—significantly below the nominal value, which should have reduced the amount of water available for incorporation into the mineral structure of the cement paste and for evaporation, thereby lessening the tendency for such cracks to develop. Yet the monolith exhibited numerous shallow, large-aperture, subvertical cracks, oriented either radial to the monolith or roughly perpendicular to lobe flow fronts, in all lifts [e.g., Lift 1, Overcore 8, Figure 3-5; Lift 2, Walter, et al. (2010, Figures 3-21 and 3-22); Lift 3, Figure 4-2], which staff interpret to have resulted from early plastic shrinkage and later hydration and drying shrinkage.

Probing this crack type, as expressed on the Lift 3 surface, indicated that these cracks terminate above the interface between Batch 6 and 7 of Lift 3 (Walter et al., 2010, Table 3-1). The pour layer in which these cracks occur was from Batch 7, to which additional water was added onsite to increase its flowability. Many of the cracks attributed to early plastic shrinkage and later hydration and drying shrinkage have orientations that are roughly perpendicular to lobe flow fronts, and given that the grout was typically emplaced in the center of the tank, such that the direction of flow was radially out from tank center, many of these cracks have radial orientations. These cracks were purposefully intersected by Corehole 6 (Walter, et al., 2010, Section 3.7; see also Figure 3-1), Corehole 8 [Figures 3-1 and 3-5(b)], and Corehole 9 [Figures 3-1 and 3-7(a),(b),(d)].

This crack type, which is related to evaporation and drying, formed in a near 100 percent relative humidity environment because the monolith was covered with an impervious plastic sheet soon after each lift was poured that remained in place for approximately 1 month after the

final pour of the final lift was emplaced. The presence of water drop impressions on the surface of the grout monolith suggests that condensation formed on the lower surface of the plastic cover, supporting staff's assumption that relative humidity inside the closed tank was 100 percent during early curing. High humidity is also expected within NDAA tanks during early curing.

All cores had a matrix color change from light tan nearest the monolith surface to gray at depths ranging from 6 to 15 cm [2.4 to 5.9 in] (e.g., Figures 3.3 and 3.6). This color change may be strongly associated with the evaporation zone where early plastic shrinkage cracking and later hydration and dying shrinkage cracking occurs. The color change is inferred to be related to weathering, including such processes as oxidation, carbonation, and capillarity migration of dissolved constituents, of the grout in close association with the atmosphere—an interpretation supported by similar light tan colors at deeper depths surrounding cracks that are open to the atmosphere [Figures 3-4(a) and 3-7(a),(b)]. An equivalent color change is not noted in the Section One and Section Three grout exposures, which suggests these surfaces were subject to atmospheric weathering and evaporative water losses—with implications for grout–tank wall bonding. Horizontal coring directed from these surfaces into the center of the grout monolith could produce cores that would be illustrative in terms of the thickness of the evaporation zone or weathering rind that surrounds the walls of the monolith.

5.5.3 Narrow-Aperture, Linear, Vertical Cracks

The intermediate-scale specimen also has at least two highly permeable (Walter, et al., 2010, Section 3.8), narrow-aperture, vertically throughgoing, linear *en echelon* cracks that penetrate multiple lifts and dissect the monolith near its center (Figures 3-6 and 4-2). The northeastern crack was intersected in Core 2 (Walter, et al., 2010, Section 3.7) and both were intersected in Overcore 9. The crack intersected by Core 2 was found to extend down through the whole length of the corehole, which was 61 cm [24 in]. The long crack intersected by Overcore 9 extended the whole length of the core, which was 77 cm [30.3 in].

These *en echelon* cracks might be interpreted as early plastic settlement and/or presetting cracks due to observation of a similarly placed linear crack within Lift 1 that developed less than 24 hours after grout emplacement and before hydration had produced elevated temperatures. The Lift 2 map of surface cracks (Walter, et al., 2010, Figure 3-20) did not show these two cracks, however, so within this lift, they had to have developed later, even if shortly thereafter. These cracks are observed to have developed subsequent to the shallow, subvertical crack intersected by Overcore 9; consequently, they might also be interpreted as late-developed settlement cracks. Thus, there is evidence to support both early formation and related causation (Walter, et al., 2010, Figure 3-7) and relatively late formation and related causation (Figure 3-7).

Two near-vertical cracks are exposed in the Lift 2 sidewall of the grout at the Section Three destructive evaluation grid; these cracks were present prior to removal of the tank wall, as evidenced by the coin-tap test results (Figures 2-7 and 3-8). The portions of the grout monolith and its containment tank in this region were likely subject to more diurnal expansion and contraction than were regions nearer the angle-iron crossbar, because the crossbar should serve to constrain expansion and contraction. The two cracks that formed within the Lift 2 sidewall within the Section Three grid are oriented consistent with the hypothesis that their development is linked to expansion and contraction within a relatively unconstrained region of the tank.

5.5.4 Cracks Induced by Coring Operations and Possibly Also by Settlement

Two vertical-to-subvertical crack families developed late and tangential to the coreholes from which Core 3 and Core 5 were extracted (Figure 4-2). The throughgoing vertical crack that developed tangential to Corehole 3 was purposefully intersected by Overcore 8 [Figures 3-5(b) and 3-6(b),(d)]. Other cracks bifurcated off the Corehole 3 crack in response to wet coring of Corehole 8. The subvertical crack family that developed tangential to Corehole 5 consists of a long series of *en echelon* cracks (Figure 4-2), one of which is exposed in cross section in the sidewall of the Section One destructive evaluation grid (Figure 3-8). These late-developed cracks/crack families, which were not present during permeability testing of Coreholes 3 and 5, are attributed to dry-coring-induced mechanical stresses, perhaps combined with diurnal tank expansion, contraction, and related differential settlement-induced stresses. The semi-parallel-to-tank-wall orientation of the crack that developed tangential to Corehole 3, combined with its location relative to the angle-iron crossbar, suggests that the formation of this crack is also potentially linked to diurnal expansion and contraction effects. Propagation of and bifurcated splitting off the Corehole 5 crack family was also observed when the Section One wall was removed for grout bonding evaluation (Figures 3-8 and 3-9). The Corehole 5 crack is clearly visible within Corehole 5 and should be further examined borescopically.

5.5.5 Annuli Surrounding Internal Fixtures and Grout–Tank Wall Debonds

Gas injection tests indicated the presence of annuli around pipes and possible (but not definitive) sub-macroscopic cracks in drum specimens, but no macroscopic cracks were observed. The same was true of the sector specimen.

For a given percentage of volumetric shrinkage, the resulting air gap surrounding fixtures will increase with the volume of the container (i.e., drum annuli<sector annuli<intermediate-scale grout monolith annuli). Shrinkage-reducing admixtures (Sant, et al., 2006) might be utilized to minimize development of annuli between grout and tank fixtures/walls, which have been observed in all grout monolith specimens.

6 MATHEMATICAL MODELS FOR PREDICTING CRACKING

Early attempts to simulate the development of cracks in large concrete structures appear to have focused on thermomechanical effects. Torrenti, et al. (1994) describe numerical simulations of stress and temperature evolution in early-age concrete with applications to large bridges. Pedersen (1994) discusses a two-dimensional finite element analysis of stress and temperature development in small (i.e., meter-scale) structures. Sato, et al. (1994) present numerical simulations of thermal stress and deformation for several types of concrete beam. Emborg and Bernander (1994) present an analytical solution for calculating two-dimensional thermal stresses in young concrete. More recent models have been expanded to three dimensions and are used to analyze complex concrete structures (e.g., Noorzaei, et al., 2009).

The recognition that hydration effects also create internal stresses leading to crack development in large concrete structures prompted Yuan and Wan (2002) to develop a combined finite element and finite difference code for analyzing early-age concrete cracking. Their model represents cracking strains due to thermal variations, drying, and the time-dependent creeping behavior of concrete. They validated their model by comparing simulated results of relative humidity and internal stresses with those measured during a controlled laboratory experiment on a 30 cm [1 ft] by 30 cm [1 ft] by 15 cm [0.5 ft] specimen. Although the simulations agreed well with the experimental data, whether or not their model could reliably simulate larger structures is uncertain. In particular, their model appears to use an elastic model to represent stress and strain relations in the structure. Such a model may be invalid once cracks develop.

The literature review for this report did not reveal any commercial computer codes specifically designed to simulate the complex processes influencing crack development in large concrete structures. A versatile finite element code, such as ABAQUS®, could possibly be used for this purpose because it is capable of modeling the thermomechanical behavior including time-dependent, inelastic stress-strain evolution (creep) and possibly the cracking process. Substantial effort, however, would be required to add more advanced material models to ABAQUS that would be capable of capturing the key aspects of the chemical evolution of curing grout.

7 POTENTIAL SIGNIFICANCE OF GROUT DEBONDING AND CRACKING FOR NDAA GROUT MONOLITHS

This chapter presents a preliminary evaluation of the significance of debonding and cracking mechanisms observed in the intermediate-scale grout monolith to grout that may be emplaced in full-scale tanks and vaults at NDAA sites.

The intermediate-scale grout monolith differs from full-scale grout-stabilized NDAA tanks in several respects, and these differences should be considered when applying staff understanding of the cracking and bonding behaviors of the intermediate-scale grout monolith to full-scale NDAA tanks. First, the physical dimensions of the intermediate-scale monolith are smaller than those of full-scale NDAA tanks. The radial dimension of the intermediate-scale monolith is approximately one-quarter that of NDAA tanks at Savannah River Site, and its height is approximately one-tenth that of NDAA tanks. These differences in dimension are likely to cause differences in (i) the density and sizes of grout spatters that adhere to tank walls and interior fixtures prior to being covered over by the larger grout mass, (ii) crack sizes and dominant cracking mechanisms, (iii) heating and cooling histories, and (iv) the scale of topographic variation at the top of each lift that is due to the mounding of grout below the injection point. Second, NDAA tanks will be fully surrounded by soil, which will reduce their rate of heat loss relative to that experienced by the intermediate-scale grout monolith, which was constructed aboveground with steel walls exposed to the atmosphere. Third, the duration of the 100 percent humidity condition to which the grout in the intermediate-scale grout monolith was exposed may have differed from conditions that will dominate in a full-scale NDAA tank during grout emplacement, and this could have affected the degree of early plastic shrinkage cracking and later hydration and drying shrinkage cracking that is observed in the monolith. Finally, the solid materials (sand, fly ash, slag, and cement) used to formulate the grout in the intermediate-scale monolith were reasonable representations of but not identical to those that will be used in full-scale NDAA grouts. Differences in materials, particularly grain size distribution and angularity of the sand, could affect the rheologic properties of the grout.

7.1 Potential for Grout Debonding

It is important for tank-waste-stabilizing grout to bond to the waste tank liner to minimize any potential for thin water films or rivulets to enter a gap between the grout mass and tank wall liner. The concern is that water films or rivulets could rapidly flow through such gaps down into the residual contamination zone at the base of the tank.

Thermal contraction during curing is thought to be the primary causative factor for poor grout–tank wall bonding, where it occurs. Other factors that may influence the quality of grout–tank wall bonds are the weight of overburden, or lack thereof, and the presence and density of preexisting grout spatter from emplacement of prior lifts. Bonds will also be affected by variability of

- Dust
- Oils
- Corrosion products
- Preexisting grout spatters

and any other residue that clings to the tank wall and internal tank fixtures. Bonding of old concrete to new concrete can be achieved by mechanically or chemically roughening surfaces, and concrete surface preparation is a well-known requirement prior to concrete repair.

Grout spatters sometimes adhere better to the grout mass and sometimes adhere better to the tank wall. No particular dominance of one condition over the other was noted. Grout spatters cause additional void space at the tank wall/fixtures where fresh bulk grout does not fully flow into open void space surrounding early-cured grout spatters.

In a full-size NDAA tank, grout spatters may not be a factor affecting the bond between grout and tank walls if the tanks are centrally filled with walls too far removed from the point of injection to receive grout spatters. But even if grout spatters are immaterial to full-size NDAA tank walls due to distance from injection point, they may affect the bonding between grout and internal tank fixtures nearer the injection point. To some degree, the effect of grout spatters could be minimized if grout were injected only below the existing fresh grout level once the fresh grout has surpassed a minimal thickness. However, no such plans are known to be in place for NDAA tank closures.

A limited review of available literature suggests there has been substantial work performed by others (especially those concerned with concrete repair) to understand and maximize concrete adhesion and bonding. Staff recommend a detailed review of the available literature to better place our nondestructive and destructive testing results for grout–tank wall bonding into proper context.

7.2 Potential for Plastic Shrinkage and Settlement and Presetting Cracking, and for Hydration and Drying Shrinkage Cracking

The cracks that staff interpret as having been caused by early plastic shrinkage, plastic settlement, and presetting and by later hydration and drying shrinkage appear to be related to/form as a result of nonlevel surface topography. DOE does not intend to use vibration to settle/densify and level each lift; thus, if the grout batch of the day is not flowable, the grout will locally mound up and potentially be more susceptible to hydration and drying shrinkage crack formation. Cracks attributed to this mechanism appear to be of limited depth, but do create connections (i.e., permeable crack networks) with larger mechanical stress cracks caused by other phenomena.

Permeability increases with water-to-cement ratios, yet higher water-to-cement ratios may be needed to improve the flowability and self-leveling capabilities of grout (Ojovan and Lee, 2005) that will not be vibrated into place. The higher the permeability of waste tank grout, the more sensitive the monolith is to aggressive groundwater and the less leach resistant it will be (Ojovan and Lee, 2005).

Voids are typically minimized and density maximized in massive concrete infrastructure through use of vibration (Yamazaki, et al., 1994; Ojovan and Lee, 2005), which also has the effect of leveling surface topography. No such plans are in place for installation of grout monoliths within NDAA tanks. In certain cases, non-self-leveling grout is even reported to be desirable in corraling certain wastes for pumped removal. Mechanical stress cracking related to uneven topography in the absence of vibration may thus be expected within NDAA waste tanks given that specifications for flowable grout do not necessarily ensure grout will be flowable enough to be self-leveling (Walter, et al., 2010).

7.3 Potential for Thermomechanical Stress Cracking

Heat of hydration and resultant large temperature gradients within massive concrete infrastructure (both reinforced and unreinforced) are of primary importance to restraint stresses

and the formation of cracks (Springenschmid, 1994), but this observation may not directly apply to the grout formulations being considered for NDAA tank closures due to the different material properties of NDAA grouts versus construction concrete. Little information was found on the thermal properties of grout materials. Most of the literature surveyed was related to the thermal conductivity of superplasticized grout used to seal boreholes and pipes for geothermal heat pump systems. Grout may be more susceptible to thermomechanical cracking than construction concrete, yet no cracks within the intermediate-scale grout monolith can be conclusively linked to the thermomechanical mechanism.

Portland cement Type IV is commonly used in massive structures when minimizing the heat of hydration is important (Ojovan and Lee, 2005) to prevent thermal stress cracking. Type IV is a low-heat cement having relatively low weight percent tricalcium silicate ($3CaO{\cdot}SiO_2$ or C_3S) and tricalcium aluminate ($3CaO{\cdot}AL_2O_3$ or C_3A), and relatively high weight percent dicalcium silicate ($2CaO{\cdot}SiO_2$ or C_2S). Ojovan and Lee (2005) recommend its use for massive waste cement monoliths. Type IV cements hydrate more slowly than all other cement types, with ultimate strength reached as late as 1 year after pouring in an environment having an average annual temperature of 20 °C [68 °F] (Ojovan and Lee, 2005). Type IV cement monoliths have a denser structure and higher long-term strength (Ojovan and Lee, 2005) than all other cement types. Type IV cements are not under consideration by those formulating grouts for NDAA tank closure.

7.4 Potential for Other Mechanical Stress Cracking

The internal and external constraints on grout monoliths produce mechanical stresses that can cause cracking when the stress field changes. NDAA grout monoliths will be externally restrained during curing by their tank liner and internally restrained by the presence of various internal fixtures. The process of debonding between grout and the tank liner and between grout and internal fixtures can potentially cause mechanical stress cracking, such as some cracks observed in the sidewall exposures of the intermediate-scale grout monolith. The steel tank liner encasing the intermediate-scale grout monolith was subject to diurnal solar heating and cooling, probably with maximum expansion/contraction occurring in the direction orthogonal to the angle-iron crossbeam, and minimum expansion/contraction occurring in the direction of the crossbeam. This expansion and contraction likely played a role in any debonding that occurred, as well as in crack formation. Buried NDAA waste tanks will not be subject to equivalent diurnal heating and cooling extremes; thus staff recommend that a new grout monolith be constructed to investigate the effect of minimized diurnal heating and cooling (as expected in an NDAA waste tank) on grout–tank wall bonds and cracking. Destructively removing two wall sections for analysis released restraining stresses and caused existing cracks to evolve and new cracks to form, but taking the action that led to development of these cracks has no direct analog to the NDAA case, although it may be similar to cracks that develop during a debonding scenario.

Cracks can also be created by external stresses such as ground settlement and seismically induced stresses. Two major throughgoing, linear, and narrow *en echelon* cracks that nearly bisect the intermediate-scale grout monolith into two equally sized halves (Figure 4-2) were interpreted as settlement cracks. Much uncertainty remains regarding the degree to which external mechanical stress will affect cracking of NDAA grout monoliths.

8 SUMMARY AND RECOMMENDATIONS

To establish a base-level understanding of the potential for fast flow pathways to form within grout soon after it is emplaced in an NDAA waste tank, CNWRA staff developed the intermediate-scale grout monolith specimen at SwRI facilities in San Antonio, Texas, as an analog to grouted tanks at NDAA facilities (Walter, et al., 2009, 2010). In fiscal year 2011, staff investigated the bonding and cracking behavior and related properties of cementitious grout in an intermediate-scale grout monolith. This grout is similar to that which may be used to stabilize NDAA waste tanks. These investigations included

- Nondestructive evaluation of the presence or lack of air gaps between the grout mass and the tank liner using ultrasonic testing and coin-tap testing
- Destructive evaluation of the interface between the grout and two discrete sections removed from the tank wall
- Observations of water breakthrough patterns on the exposed grout wall following water injection during wet-coring operations
- Measurements and descriptions of the two exposed grout wall sections and three extracted cores, including the presence and characteristics of horizontal partings and vertical-to-subvertical cracks
- High-resolution laser measurements of the surface topography of the grout monolith and detailed mapping and geographic information systems-based analysis of variable crack apertures, crack frequencies, and crack types on its surface
- Synthesis of literature describing cracking mechanisms in large concrete infrastructure and interpretation of observed grout monolith cracks in terms of known cracking mechanisms
- A brief literature review of numerical modeling work undertaken by others that might form a foundation from which to begin NDAA-focused modeling to better understand key factors affecting the formation of cracks in grout monoliths
- Interpretation of the potential significances of bonding and cracking for NDAA grout monoliths

8.1 Observations and Findings Related to the Intermediate-Scale Grout Monolith

Ultrasonic and coin-tap nondestructive testing methods were used to investigate the bond between the grout and the tank liner (i.e., the wall) of the intermediate-scale grout monolith. Based upon comparison of the ultrasonic inspection results with the destructive testing of two sections of the intermediate-scale grout monolith's tank wall, it appears that the zero degree, longitudinal ultrasonic technique provided a good means to determine whether the interface between the grout and the tank wall was affected by the presence of an air gap. While the presence of an air gap is strongly suggestive of a debonded condition, the lack of an air gap does not conclusively prove that a bond exists between the grout and the tank liner or wall. Because the coin-tap test is only capable of identifying larger voids, this test method did not

prove reliable for detecting small air gaps that were positively identified by the ultrasonic method. However, it was useful for identifying the presence of near-surface air gaps located behind near-vertical cracks at the grout–tank wall interface.

DSI imaging and high-resolution photographic methods were used to investigate the grout residue that remained adhered to two destructively removed sections of the tank wall. Results provide insight into the nature of the interface between tank wall and grout. Observations indicate that bonding of the grout to the tank wall is not uniform. As grout was emplaced in the intermediate-scale grout monolith, grout commonly spattered onto the tank liner above the existing grout level and during later pours was covered over by the emplaced bulk grout mass. Destructive removal of two tank wall sections illustrated that these early cured grout spatters sometimes adhere well to the tank wall and sometimes remain with the grout mass. Although spatter can adhere to the tank wall, the bulk grout mass may not adhere well to the spatter, with the result that a vertical discontinuity exists within a few millimeters of the tank wall. Though not a crack *sensu stricto*, the discontinuity may appear and act as a crack. Because grout emplaced within the monolith was not vibrated to enhance compaction and leveling and to eliminate the presence of air bubbles, the presence of grout spatter on tank walls leads to additional pore space surrounding each spatter because freshly poured bulk grout tends to not flow into all available void space surrounding early-cured grout spatters.

Destructive removal of the two tank wall sections changed the stress state within the monolith, causing existing cracks to evolve and new cracks to develop with time. Grout within lower lifts tends to be smoother than grout within the uppermost lift, which is attributed to the role played by overburden pressure that tends to compress voids, vesicles, vugs, and air bubbles in the lower lifts of grout. Interface quality between the three lifts was variable, with grout at an interface either tending to remain with the grout mass or tending to adhere to the removed tank liner sections.

Observations of epoxy uptake by crack systems and wet-coring water that seeped from the exposed sides of the intermediate-scale grout monolith indicate the presence of an extensive network of permeable pathways through the specimen.

Features revealed through extraction of cores ranged from matrix color variations to vug sizes, crack distributions, apertures, and trace lengths. Matrix color change at a consistent depth below the surface of the grout is interpreted to indicate the vertical extent of the evaporation zone, within which water is transferred to the atmosphere and early plastic shrinkage cracks and later hydration and drying shrinkage cracks form. Excess porosity is present in the form of vesicles and vugs because the grout was not vibrated subsequent to emplacement. The three extracted cores provide evidence that various material components or grout ingredients were not completely mixed at the batch plant or during delivery to the site, leaving some vugs partly filled with friable particulate matter. Cracks are sometimes observed to penetrate relatively soft clasts instead of forming around clast edges. Horizontal crack intensity, as estimated from vertical cores, is four to seven cracks per meter [one to two cracks per foot]. Vertical and subvertical cracks, however, are undersampled by vertical core and are best understood at this time from an analysis of cracks intersecting the grout surface.

Staff further characterized the 218 cracks exposed on the surface of the intermediate-scale grout monolith by mapping their locations and variable apertures. Cracks are distributed in fairly distinct sets, including (i) radial to the monolith, (ii) roughly perpendicular to lobe flow fronts, (iii) two *en echelon* cracks that nearly bisect the monolith into equal halves, and (iv) a few cracks/crack families concentric to the monolith edge. Crack aperture varied from <0.5 to 8 mm

[<0.02 to 0.31 in], with variation in aperture along crack length. Aperture values of at least 4 mm [0.16 in] were found in each quadrant of the monolith. Crack frequency, computed for 12 equal areas on the surface of the monolith, ranged from 1 to 26 cracks per square meter [9.3×10^{-2} to 2.4 cracks per square foot]. Crack frequency is highest within the mounded grout flow lobes. The center of the grout monolith, where grout was preferentially pumped, is 21.9 cm [8.6 in] higher than the lowest point in the northeast quadrant of the tank, and topography is correlated to crack distribution, with higher crack frequency in areas of higher topography. Many cracks terminate at or near the edge of mounded grout flow lobes.

8.2 Summary of Literature Review of Cracking Mechanisms

Concrete literature is vague regarding measureable crack characteristics that would allow definitive determination of cracking mechanisms, and some cracks may reflect a combined response to more than one cracking mechanism.

Plastic shrinkage, plastic settlement, and presetting cracks are related to contraction due to early water loss (i.e., evaporation from a free surface). Hydration and drying shrinkage occurs later during the curing process by incorporation of water molecules into the mineral structure of the cement paste and by loss of water to evaporation at the concrete surface. Drying shrinkage is commonly of minor importance to formation of cracks in massive concrete infrastructure (Springenschmid, 1994), but this may be due to common use of vibration or other compaction mechanisms that have no bearing on NDAA tank closure. Plastic shrinkage, plastic settlement, and presetting cracking and hydration and drying shrinkage cracking are interpreted to have played a major role in the development of numerous, relatively shallow but wide-aperture subvertical cracks in multiple lifts within the intermediate-scale grout monolith. These cracks formed in a near 100 percent relative humidity environment because the monolith was covered with an impervious plastic sheet for approximately 1 month after the final pour of the final lift was emplaced. High humidity is also expected within NDAA tanks during early curing.

Heat of hydration and resultant large temperature gradients within massive concrete infrastructure (both reinforced and unreinforced) are of primary importance to restraint stresses and the formation of cracks (Springenschmid, 1994), but this observation may not directly apply to the grout formulations being considered for NDAA tank closures due to the different material properties of grout versus construction concrete. Little information was found on the thermal properties of grout-type materials. Most of the literature surveyed was related to the thermal conductivity of superplasticized grout used to seal boreholes and pipes for geothermal heat pump systems. Allan (2000) reported the coefficient of thermal expansion of superplasticized cement–sand grout formulation designed for sealing such pipes was 1.65×10^{-5}/°C [0.92×10^{-5}/°F], approximately 60 percent greater than that of typical construction concrete and similar to neat cement. Thus, grout may be more susceptible to thermomechanical cracking than construction concrete, yet to date, no cracks within the intermediate-scale grout monolith can be conclusively linked to the thermomechanical mechanism.

Cracking is also influenced by the internal and external constraints on the grout; that is, by the boundary conditions provided by the structure that restrains the grout during the thermal expansion stage. Expansion cracks that form during the heating phase tend to close as the structure cools and to not be throughgoing, whereas cracks that form during the cooling phase tend to remain open and be throughgoing. The intermediate-scale grout monolith was restrained during curing by its tank liner and also by the angle-iron crossbeam where the two halves of the tank were joined together. The restraint provided by this crossbeam may have no direct analogy to most NDDA waste tanks, and no cracks within the intermediate-scale grout

monolith have been conclusively linked to expansion cracks that formed during the early curing phase.

Cracks can also be created by external stresses after the structure has cooled, such as ground settling, deformation of bounding constraints, and seismically induced stresses. Two throughgoing, linear, and narrow *en echelon* cracks that nearly bisect the monolith into two equally sized halves are interpreted as settlement cracks. Destructively removing two wall sections for analysis released restraining stresses and caused existing cracks to evolve and new cracks to form, but taking the action that led to development of these cracks has no direct analog to the NDAA case. The steel tank liner encasing the grout monolith was subject to diurnal solar heating and cooling, probably with maximum expansion/contraction occurring in the direction orthogonal to the angle-iron crossbeam, with minimum expansion/contraction occurring in the direction of the crossbeam. Buried NDAA waste tanks will not be subject to equivalent diurnal heating and cooling extremes. Much uncertainty remains regarding the degree to which external mechanical stress will affect cracking of NDAA grout monoliths.

The literature review for this report did not reveal any commercial computer codes specifically designed to simulate the complex processes influencing crack developed in large concrete structures. A versatile finite element code, such as ABAQUS, could possibly be used for this purpose because it is capable of modeling the thermomechanical behavior including time-dependent, inelastic stress-strain evolution (creep) and possibly the cracking process. Substantial effort, however, would be required to add more advanced material models to ABAQUS that would be capable of capturing the key aspects of the chemical evolution of curing grout.

8.3 Future Work and Recommendations

Cracks were observed to continue to propagate within the intermediate-scale grout monolith during the period of this investigation. Air gap apertures between the grout mass and internal tank fixtures also evolve with curing time, as demonstrated with the initial set of 12 drum grout specimens and the sector specimen (Walter, et al., 2010). The porosity of a hydrating cement paste decreases with time. The permeability of a newly constructed monolith decreases with porosity but increases with the development of micro- and macrocracks. Early permeability values were estimated for the intermediate-scale grout monolith in fiscal year 2010 (Walter, et al., 2010), but permeabilities that would account for parameter evolution as a function of cure time have not been reestimated since that time. Thus, staff recommend pneumatic retesting of the grout monolith.

As of the date of this report, gas injection testing of fiscal year 2010 drum grout specimens of surrogate Idaho National Laboratory heel grout and South Carolina reducing grout remains to be performed. These tests could only have been performed after allowing at least 30 days of curing of the specimens in 2010, but there was no funding available to support this work in fiscal year 2010, nor were these tests included in the fiscal year 2011 operations plan. Thus, staff also recommend that pneumatic testing of the fiscal year 2010 drum grout specimens of surrogate Idaho National Laboratory heel grout and surrogate Savannah River Site reducing grout be performed in fiscal year 2012.

The behavior and characteristics of the intermediate-scale grout monolith indicate that relatively large grout specimens are required to understand the flow behavior and cured properties of the grout that may be placed in the NDAA tanks. Further characterization of the intermediate-scale grout monolith is recommended to include

- Borescopic observations and descriptions of cracks exposed in sidewalls of Coreholes 1–9 (Coreholes 3 and 5, in particular, are known to have developed cracks after core removal; furthermore, the upper half of Corehole 8 has large cracks filled with epoxy from which additional information can be gleaned that was not easily discernable from its broken overcore)

- Volumetric measurement of epoxy applied to/accepted by any future coreholes as an estimate of local crack porosity

- Controlled-volume tracer experiments, with rapid time-lapse photography or videography used to record breakthrough times and styles

- Thin section preparation and analysis to understand the characteristics of strong versus weak aggregate particles (i.e., those which cracks penetrate through rather than traverse around), and clumps of poorly mixed ingredients

- Horizontal coring from exposed sidewalls into the center of the monolith to better capture the frequency of hydraulically important vertical cracks, which are undersampled by vertical cores [horizontal cores would also likely reveal the thickness of the weathering rind/evaporation zone (through matrix color change) that is anticipated to surround the perimeter of the grout monolith]

New grout monoliths can be constructed to

- Investigate the effect of minimized diurnal heating and cooling (as expected in an NDAA waste tank) on grout–tank wall bonds

- Investigate the effect of humid condition duration on development of early plastic shrinkage and later hydration and drying shrinkage cracks

- Measure mechanical and thermal stresses during curing and record the timing of crack formation, where the timing of formation is diagnostic of formation mechanism

When additional experimental grout monoliths are constructed under this program, staff recommend that separate pours within each lift be dyed different colors to aid identification, because some lift separations and hiatuses between pours are difficult to identify in cores.

A brief review of available literature suggests there has been substantial work performed by others who are concerned with concrete repair to understand concrete adhesion and bonding. Staff recommend a detailed review of the available literature to better place our nondestructive and destructive testing results for grout–tank wall bonding into proper context.

Finally, degradation characteristics and leach resistance of engineered analogs from the low-level waste and transuranic (intermediate-level) waste programs of various nations might be examined under this program in the future, with the caveat that emplacement mechanisms differ in significant ways, and thus material and chemical properties may also differ to significant degrees.

9 REFERENCES

Allan, M.L. "Materials Characterization of Superplasticized Cement-Sand Grout." *Cement and Concrete Research.* Vol. 30, No. 6. pp. 937–942. 2000.

Bernander, S. and M. Emborg. "Risk of Cracking in Massive Concrete Structures—New Developments and Experiences." *Thermal Cracking in Concrete at Early Ages*. R. Springenschmid, ed. Spon, London: E&FN. pp. 385–392. 1994.

Emborg, M. and S. Bernander. "Thermal Stress Computed by a Method for Manual Calculations." *Thermal Cracking in Concrete at Early Ages*. R. Springenschmid, ed. Spon, London: E&FN. . pp. 321–328. 1994.

Franke, E.A., M.J. Magee, J.N. Mitchell, and M.P. Rigney. "3D Precision Surface Measurement by Dynamic Structured Light." Presented at and published in the Proceedings of the Society of Photo-Optical Instrumentation Engineers Photonics East Conference, Providence, Rhode Island, October 2003.

Hsum, D.K., D.J. Barnard, and D.P. Roach. "Tap Test: Evolution of an Old Technique, Back to Basics: Nondestructive Materials Testing." *Quality Magazine.* Vol. 67, No. 7. pp. 785–791. July 2009.

Light, G., S. Winterberg, and C.L. Dinwiddie. "NDE Evaluation of Bonding to Large Grout Tank." Scientific Notebook 1074 & CD. San Antonio, Texas: CNWRA. pp. 1–33. 2011.

Neville, A.M. *Properties of Concrete*. Fourth edition. New York City, New York: John Wiley & Sons. 844 pp. 1996.

Noorzaei, J., K.H. Bayagoob, A.A. Abdulrazeg, M.S. Jaafar, and T.A. Mohammed. "Three Dimensional Nonlinear Temperature and Structural Analysis of Roller Compacted Concrete Dam." *Computer Modeling in Engineering & Sciences.* Vol. 47, No. 1. pp. 43–60. 2009.

Ojovan, M.I. and W.E. Lee. "Chapter 15—Immobilisation of Radioactive Wastes in Cement." *An Introduction to Nuclear Waste Immobilisation*. Amsterdam, The Netherlands: Elsevier. 2005.

Pedersen, E.S. "Prediction of Temperature and Stress Development in Concrete Structures." *Thermal Cracking in Concrete at Early Ages.* R. Springenschmid, ed. Spon, London: E&FN. pp. 297–304. 1994.

Sant, G., F. Rajabipour, P. Lura, and W.J. Weiss. "Examining Time Zero and Early-Age Expansions in Pastes Containing Shrinkage Reducing Admixtures (SRAs)." Proceedings of the 2nd RILEM Symposium on Advances in Concrete Through Science and Engineering, RILEM, Quebec City, Canada. 2006.

Sato, R., W.H. Dilger, and I. Ujike. "Deformations and Thermal Stresses of Concrete Beams Constructed in Two Stages." *Thermal Cracking in Concrete at Early Ages.* R. Springenschmid, ed. Spon, London: E&FN. pp. 313–320. 1994.

Springenschmid, R., ed. "Preface." *Thermal Cracking in Concrete at Early Ages*. Spon, London: E&FN. 1994.

Torrenti, J.M., F. de Larrard, F. Guerrier, P. Acker, and G. Grenier. "Numerical Simulation of Temperatures and Stresses in Concrete at Early Ages: The French Experience." *Thermal Cracking in Concrete at Early Ages.* R. Springenschmid, ed. Spon, London: E&FN. pp. 281–288. 1994.

Walter, G.R. and C.L. Dinwiddie. "Conceptual Design for Small-Scale Grout Monolith Tests." San Antonio, Texas: CNWRA. April 2008.

Walter, G.R., C.L. Dinwiddie, D. Bannon, G. Frels, and G. Bird. "Intermediate Scale Grout Monolith and Additional Mesoscale Grout Monolith Experiments: Results and Recommendations." Status Report. San Antonio, Texas: CNWRA. September 2010.

Walter, G.R., C.L. Dinwiddie, E.J. Beverly, D. Bannon, D. Waiting, and G. Bird. "Mesoscale Grout Monolith Experiments: Results and Recommendations." San Antonio, Texas: CNWRA. July 2009.

Yamazaki, M., H. Harada, and T. Tochigi. "Low-Heat Portland Cement Used for Silo Foundation Mat—Temperatures and Stresses Measured and Analyzed." *Thermal Cracking in Concrete at Early Ages*. R. Springenschmid, ed. Spon, London: E&FN. 1994.

Yuan, Y. and Z.L. Wan. "Prediction of Cracking Within Early-Age Concrete Due to Thermal, Drying and Creep Behavior." *Cement and Concrete Research*. Vol. 32. pp. 1,053–1,059. 2002.